Cerebral Cortex, May 2018;28: 1857–1865

doi: 10.1093/cercor/bhy003
Advance Access Publication Date: 27 February 2018
Original Article

ORIGINAL ARTICLE

The Temporal Dynamics of Brain Plasticity in Aging

Ann-Marie Glasø de Lange[1], Anne Cecilie Sjøli Bråthen[1], Darius A. Rohani[1], Anders M. Fjell[1,2] and Kristine B. Walhovd[1,2]

[1]Center for Lifespan Changes in Brain and Cognition, Department of Psychology, University of Oslo, 0317 Oslo, Norway and [2]Department of Radiology and Nuclear Medicine, Oslo University Hospital, 0372 Oslo, Norway

Address correspondence to Ann-Marie Glasø de Lange, Department of Psychology, University of Oslo, Pb. 1094 Blindern, 0317 Oslo, Norway, Email: a.m.g.d.lange@psykologi.uio.no

Abstract

Cognitive training has been suggested as a possible remediation of decline in brain structure with older age. However, it is unknown whether training effects are transient or enduring, as no studies have examined training-induced plasticity relative to decline in older adults across extended periods with multiple intervention phases. We investigated the temporal dynamics of brain plasticity across periods on and off memory training, hypothesizing that (1) a decline in white matter (WM) microstructure would be observed across the duration of the study and (2) that periods of memory training would moderate the WM microstructural decline. In total, 107 older adults followed a 40-week program, including 2 training periods separated by periods with no intervention. The general decline in WM microstructure observed across the duration of the study was moderated following the training periods, demonstrating that cognitive training may mitigate age-related brain deterioration. The training-related improvements were estimated to subside over time, indicating that continuous training may be a premise for the enduring attenuation of neural decline. Memory improvements were largely maintained after the initial training period, and may thus not rely on continuous training to the same degree as WM microstructure.

Key words: aging, cognitive training, memory, plasticity, white matter microstructure

Introduction

Experience-dependent brain plasticity is well documented in both young and older adults (Draganski et al. 2004; Boyke et al. 2008; Scholz et al. 2009). Targeted cognitive training has thus been suggested as a possible remediation of decline in brain structure with older age. Although the evidence for a lifelong potential for plasticity provides a promising outlook, the premises for, and limitations of, plasticity is far from fully understood. Studies of young adults indicate that neural alterations do not persist in the absence of exercise (Draganski et al. 2004), and that structural changes recede during subsequent training on the same skill (Driemeyer et al. 2008). Thus, training effects may not last beyond the intervention periods, and the learning of new skills may be more effective for the mitigation of decline relative to sustained training on the same tasks. In older adults, brain aging itself is likely to influence the time course of plasticity, such that training effects need to be measured in relation to general decline over time. However, no studies have examined training-induced plasticity relative to decline in older adults across extended periods with multiple intervention phases. Hence, it is unknown whether repeated cognitive interventions can systematically moderate the magnitude of brain deterioration in aging, and whether continuous training is a premise for the attenuation of neural decline. White matter (WM) microstructure is highly susceptible to age-related deterioration (Sexton et al. 2014; Bender et al. 2016), and short-term changes in WM have been observed across periods of less than 3 months in healthy older adults (Engvig et al. 2012). Can WM trajectories be modified, and if so, by what means?

Evidence suggests that both young and older adults can benefit from memory strategy training (Cavallini et al. 2003; Engvig et al. 2012; de Lange et al. 2017). As this type of training has been shown to influence WM microstructure in older adults (Engvig et al. 2012; de Lange et al. 2017), we investigated whether periods of memory strategy training could modify trajectories of WM decline in 107 older adults (mean age ± SD = 73.2 ± 2.9), by using an ABAB/BABA design as illustrated in Figure 1. The training aimed to improve serial verbal recollection memory by implementing the mnemonic technique Method of Loci (MoL). An active control group focusing on popular science was included during the first 10-week period to investigate the specificity of the memory-training effects. All participants were examined with magnetic resonance imaging (MRI) and cognitive testing, with a 10-week interval between each assessment. Microstructural changes were measured using the diffusion tensor imaging (DTI) derived metrics fractional anisotropy (FA), mean diffusivity (MD), radial diffusivity (RD), and axial diffusivity (AD). We hypothesized that (1) a decline in WM microstructure would be observed over 40 weeks, (2) memory training would moderate the WM microstructural decline, and (3) training effects on WM microstructure would subside in the absence of training, but (4) would be reinvoked with a new training period.

Materials and Methods

Sample

The sample was drawn from the project "Neurocognitive Plasticity" at the Center for Lifespan Changes in Brain and Cognition (LCBC), Department of Psychology, University of Oslo. All procedures were approved by the Regional Ethical Committee of Southern Norway, and written consent was obtained from all participants. Participants were recruited through newspaper and webpage adverts, and were screened with a health interview. Participants were required to be between 70 and 80 years old, healthy adults, right handed, fluent Norwegian speakers, and have normal or corrected to normal vision and hearing. Exclusion criteria were history of injury or disease known to affect central nervous system (CNS) function, including neurological or psychiatric illness or serious head trauma, being under psychiatric treatment, use of psychoactive drugs known to affect CNS functioning, and MRI contraindications. All scans were evaluated by a neuroradiologist and deemed to be free of significant injuries or conditions. For inclusion in the study, participants were required to score ≥ 26 on the Mini Mental State Examination (MMSE) (Folstein et al. 1975) and have scores less than 2 standard deviations below mean on the 5 min delayed recall subtest of the California Verbal Learning Test II (CVLT II) (Delis et al. 2000). Three individuals were excluded based on these criteria. All participants further had to achieve an IQ above 85 on the Wechsler Abbreviated Scale of Intelligence (WASI) (Wechsler 1999). A total of 125 participants fulfilled the inclusion criteria. Sample demographics are shown in Table 1.

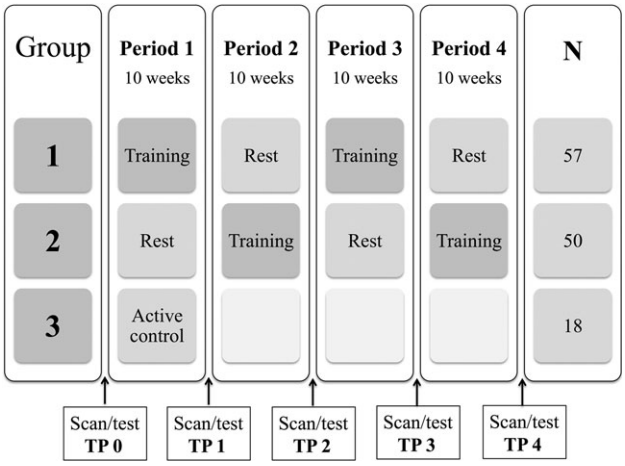

Figure 1. The course of the training program depicted for each of the 3 groups. In total, 71 participants completed the full study. Drop-out rates are provided in the Supplementary Material.

Design and Training Intervention

Pools of around 20 participants were recruited at a time, and the participants were assigned to 1 of 3 intervention groups at registration. The data collection was on-going and continuous for the 3 conditions simultaneously, ensuring that participants from all 3 experimental groups were scanned and tested interchangeably and thus reducing the possibility of group differences with regard to the assessment and scanning conditions. Although group assignments based on date do not comply with suggested criteria for randomization of participants (Schulz and Grimes, 2002), practical considerations forced a compromise due to the extensive data collection with strict time intervals and assessments locked to specific dates across 40 weeks. Group 1 (ABAB) started with 10 weeks of memory training ($N = 57$), and moved on to a subsequent rest period with no intervention followed by a second training period, and then a final rest period. Group 2 (BABA) started with 10 weeks of rest ($N = 50$), and moved on to the first training period followed by a rest period and a subsequent training period. The participants allocated to groups 1 and 2 completed scanning and cognitive testing at 5 occasions, with a 10-week interval between the assessment sessions. An active control group (group 3, AC, $N = 18$) was included during the first period in order to investigate the specific cognitive effects of the memory training. The active control participants completed scanning and cognitive testing at 2 occasions, with a 10-week interval between the assessment sessions.

The memory-training program aimed at improving serial verbal recollection memory by implementing the mnemonic technique MoL (Bower 1970), which has been shown to improve serial recall substantially in older adults (Engvig et al. 2010; de Lange et al. 2016). The training program included a single course session each week and home assignments involving memorizing word lists. The first group session included a presentation of the project, an introduction to the MoL with instructions, and an initial word list task consisting of 15 words. The following weekly group sessions included updating of the strategy, clarification of instructions and a word list task, which was increased by 5 words each week to ensure a continuous challenge. However, the participants were encouraged to individually adjust the difficulty level, with the aim of achieving a challenging but manageable training level across all the participants. Individual adjustment involved increasing/decreasing the number of words on the tasks to a sufficiently challenging level, performing the tasks within individual time limits and recollection of the word lists in reverse order. Although the exact number of words was subject to individual adjustment, all participants completed the training with a weekly increase in number of words. Eight home assignments were sent out weekly, with a minimum requirement that 4 be

Table 1 Sample demographics.

	Group 1 ABAB (28 F/29 M) M ± SD	Group 2 BABA (34 F/16 M) M ± SD	Group 3 AC (11 F/7 M) M ± SD
Age	72.8 ± 2.6	73.5 ± 3.2	73.5 ± 2.9
Education	15.4 ± 3.6	14.2 ± 2.6	16.2 ± 2.7
MMSE	28.6 ± 1.3	28.8 ± 1.1	28.2 ± 1.5
IQ	120.3 ± 11.8	117.8 ± 10.9	121.3 ± 5.6
CVLT learning	45.7 ± 10.9	46.6 ± 10.5	50.0 ± 10
CVLT recall	9.7 ± 3.5	9.8 ± 2.8	11.4 ± 3.3
MRI scan interval (days)	75.8 ± 8.3	76.6 ± 3.1	77.3 ± 1.2

Group 1 (ABAB) started with a training period, while Group 2 (BABA) started with a rest period. Group 3 (AC) completed the active control program. A one-way analysis of variance (Bonferroni corrected) showed no differences between the groups on the above measures.

completed. The home assignments consisted of word lists with various themes and followed the level of difficulty set in the group session the same week. The tasks included options for individual adjustment including increasing/decreasing the number of words, performing the tasks within individual time limits and recollection of the word lists in reverse order. The home assignments were completed online. All responses in addition to time spent on the tasks were registered to a database. The proportion of tasks completed across participants was 74% during the first training period, and 69% during the second period. The 2 training periods followed the same structure and included the same strategy training. The initial level of difficulty in the second training period corresponded to the middle level of the first period. The weekly increase in number of words in the lists was doubled during the last 3 weeks of the second training period. Thus, the final level of difficulty was higher in the second training period. The participants were instructed not to practice any memory training in the rest periods. The active control group program involved popular scientific lectures once a week. Eight home assignments were sent out weekly. The home assignments were completed online, and involved tasks related to the weekly popular scientific themes. The proportion of tasks completed across participants in the active control group was 70%. None of the tasks or lectures in the active control program involved any specific form of memory training. Contact with staff, group meetings and the number of tasks were matched between the training group and the active control group. Independent sample *t*-tests (2-sided) showed that the number of tasks completed did not differ between the training group and the active control group (mean ± SD = 57.6 ± 15.1 (range = 76) for the training group, and 55.5 ± 21.1 (range = 72) for the active control group, $t(60) = -0.45$ $P = 0.7$). We have recently investigated the influence of number of tasks completed on memory improvement and WM microstructure in the same sample. Number of tasks did not influence memory improvement or WM microstructural change during the first 10-week period (de Lange et al. 2017). Test sessions and time intervals were held identical for all participants, in order to ensure that test–retest effects would not differ across the groups.

Image Acquisition and Data Processing

A Siemens Skyra 3 T MRI scanner with a 24-channel head-coil was used (Siemens Medical Solutions; Erlangen, Germany). A diffusion-weighted echo-planar imaging (EPI) sequence was applied for each subject (FOV_{xy} = 252 × 256 mm, dimensions = 128 × 130 × 70, voxel size = 1.9626 × 1.9626 mm^2, slice thickness = 2 mm, repetition time = 9300 ms, echo time = 87 ms). Overall, 64 unique diffusion-weighted volumes were collected at *b*-value = 1000 s mm^{-2} in addition to 2 nondiffusion-weighted (*b*-value = 0 s mm^{-2}) volumes, one acquired with an opposite k-space traversal direction for the purpose of correcting susceptibility artefacts. All scan-sets were manually checked for gross motion artefacts. The susceptibility-induced field was estimated using the FSL tool topup (Andersson et al. 2003) and corrected for along with subject motion and eddy current-induced fields using the eddy tool (Andersson and Sotiropoulos 2016). Signal dropout caused by subject motion during the diffusion encoding was detected and corrected using the eddy tool, as implemented in FSL (Andersson and Sotiropoulos 2016). Each acquired slice was compared with a model free prediction, and if the observed signal was statistically different (3 standard deviations) from the prediction, it was replaced by the latter. An average of 0.38, 0.38, and 0.40 slices per volume across subjects were replaced in groups 1, 2, and 3, respectively. The number of slices replaced did not differ between groups (one-way analysis of variance, $F(2, 467) = 0.23$ $P = 0.79$). Nonbrain tissue (skull, etc.) was removed using Brain Extraction Tool (Smith 2002), employing a mask based on the nondiffusion-weighted volume. FA images were created by fitting a tensor model to the preprocessed diffusion data using FMRIB's Diffusion Toolbox (FDT) (Behrens et al. 2003). All participants' FA data were then processed with the FSL software package TBSS (Smith et al. 2006). TBSS is documented to be relatively robust to potential partial volume effects, as it assesses diffusion indices only in the estimated centers of WM tracts (Smith et al. 2006; Berlot et al. 2014). The subjects FA images were aligned into a common space using the nonlinear registration tool FNIRT (Andersson et al. 2010) which uses a b-spline representation of the registration warp field (Rueckert et al. 1999). Next, the mean FA image was calculated and thinned to create a mean FA skeleton, which represents the centers of all tracts common to the group. The threshold for the mean FA skeleton was set at 0.2, resulting in a mask of 137 832 voxels. Each participant's aligned FA data were then projected onto this skeleton. The nonlinear warps and skeleton projection stages were repeated using the MD, RD, and AD measures.

Statistical Analyses

The Time Course of WM Microstructural Changes

For each subject at every time point, the average MD, RD, AD, and FA values were calculated within the mean FA skeleton mask. The time course of WM microstructural changes was analyzed using a nonlinear mixed effects model, using the default covariance pattern (http://uk.mathworks.com/help/

stats/nlmefit) as implemented in Matlab. The model applied a continuous function to describe the estimated time course of WM microstructural changes across the duration of the study. Training effects were modeled as improvements relative to a general decline over time, in contrast to modeling each interval as a separate slope. This approach was chosen to enable an overall description of the entire trajectory including both age-related changes and training effects. The function used to describe the time course of microstructural changes is provided below. For simplicity, we refer only to MD in the text.

$$\mathrm{MD}(t) = \beta_0 + \beta_1 \times t + \beta_2 \times e^{-(t-\beta_3)^2} + \beta_4 \times e^{-(t-\beta_5)^2} + \beta_6 \times \mathrm{age} + \beta_7 \times \mathrm{sex} + \beta_8 \times \mathrm{motion} \quad (1)$$

Several terms appear in this expression, each of which describe different characteristics of MD evolution (t = time). The first term β_0 is an intercept, describing the value of MD at the beginning of the study (time point 0). This term was modeled as the sum of a fixed effect and a random effect for each subject, describing an overall group effect while allowing for individual variation in baseline MD across subjects. The second term β_1 models a linear change in MD over the duration of the study. The terms β_2 and β_4 model improvements in MD relative to the estimated linear change in MD (β_1). These improvements can occur at any time between time points 1 and 5, and be either positive or negative. β_3 and β_5 model the times at which the improvement phases occur. β_1, β_2, and β_4 were modeled as the sum of a fixed effect and a random effect, allowing both the slope and the improvements to vary across subjects. The remaining beta terms modeled the fixed effects of age, sex, and motion across all time points, and were included to account for variation in WM microstructure as a function of these variables. Motion was estimated as the mean of the average Root Mean Square displacement value across each diffusion-weighted volume derived from the eddy procedure (Andersson and Sotiropoulos 2016). Missing data were handled within the Matlab LME framework using the method of Little and Rubin (Little and Rubin 2014). In general, the nonlinear model was shown to improve with the inclusion of β_2 and β_4 relative to a more basic model describing only the intercept (β_0) and slope (β_1) (increased log-likelihood, and AIC differences > 2 (Burnham and Anderson 2003), despite the loss of degrees of freedom in the more complex model (425 vs. 419). For MD, the log-likelihood increased from 4184.1 to 4185.4, and the Akaike information criteria (AIC) decreased from −8339.1 to −8342.8. For FA, the log-likelihood increased from 1492.7 to 1499.9, and the AIC decreased from −2971.8 to −2969.4).

To investigate whether the general WM trajectories across the duration of the study resembled the WM changes observed in normal aging, we compared the estimated annual percentage change in the current sample with the annual percentage change in an independent nontraining sample of older adults, who were followed for a substantially longer interval of 3.2 years (N = 38). An independent samples *t*-test (2-sided) was used to compare the change in the current sample to the change in the matched sample (sample details and results are provided in the Supplementary Material).

Memory Improvement

Memory performance was measured using an experimental word-list test developed to measure verbal recollection. The test enabled the MoL to be applied, such that the measure of memory performance was closely related to the utilized technique, and thus convenient for measuring training gains (see de Lange et al. (2017) for details). The total number of words recalled from the word-list test was used as the measure of memory performance. In a similar fashion to microstructural changes, memory trajectories were analyzed using a nonlinear mixed effects (NLME) model, as implemented in Matlab. First, improvements relative to the intercept were estimated across the duration of the study, using the following function:

$$\mathrm{Memory}(t) = \beta_0 + \beta_1 \times e^{-(t-\beta_2)^2} + \beta_3 \times e^{-(t-\beta_4)^2} + \beta_5 \times \mathrm{age} + \beta_6 \times \mathrm{sex} \quad (2)$$

The terms β_1 and β_3 model changes in memory performance relative to the intercept (β_0), while β_2 and β_4 model the times at which the changes occur. The intercept (β_0) and improvement phases (β_1 and β_3) were modeled as random factors. The remaining beta terms model the fixed effects of age and sex across all time points. Next, we calculated the difference between the estimated performance at the time points of improvement and the estimated performance before each improvement phase.

To assess possible transfer effects during the first 10-week period, repeated measure ANCOVAs were run using intervention group as between-subject factor, and change in performance on the following tests as dependent variables: The Wechsler Digit Span test, a working memory test where the participants were asked to render a sequence of numbers forward and backward, the Rey–Osterrieth Complex figure test (RCFT), measuring visual recollection (Lezak 2004), an experimentally developed paired-words test, where the participants were asked to recall pairs of unassociated words, and the CVLT learning and recall trials. The memory training did not influence performance on the Digit Span test, the RCFT or the paired-words test. However, performance on the CVLT learning and 30-min recall improved to a larger extent in the training group relative to the control group, reflecting a near-transfer effect. The results are provided in the Supplementary Material.

Results

The Time Course of Microstructural Changes

The time course of MD is shown in Figure 2. The slope function (β_1) estimated a positive slope, indicating a general increase in MD across the duration of the study. An improvement in MD

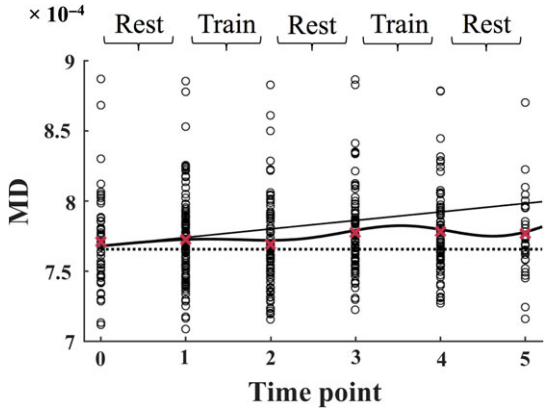

Figure 2. The MD values for each subject (total *n* = 107) are plotted separately at each time point. The slope is displayed as a solid line, and the mean values across all subjects are displayed as red crosses. The full model is displayed as a solid curved line. The dotted line marks the intercept of the model at time point 0. The data is modeled according to Equation 1 (see Materials and Methods). MD = mean diffusivity.

Table 2 WM microstructure results.

WM	Parameter	Description	Value ± SE	F(1, 419)	P
MD	β_1	Slope	$(6.21 \pm 1.77) \times 10^{-6}$	12.29	5.03×10^{-4}
	β_2	Improvement phase 1	$(-9.54 \pm 4.05) \times 10^{-6}$	5.54	0.02
	β_4	Improvement phase 2	$(-21.70 \pm 8.79) \times 10^{-6}$	6.10	0.01
AD	β_1	Slope	$(6.63 \pm 1.35) \times 10^{-6}$	8.00	0.01
	β_2	Improvement phase 1	$(-1.07 \pm 0.52) \times 10^{-5}$	4.19	0.04
	β_4	Improvement phase 2	$(-2.34 \pm 1.14) \times 10^{-5}$	4.15	0.04
RD	β_1	Slope	$(5.96 \pm 1.56) \times 10^{-6}$	14.63	1.51×10^{-4}
	β_2	Improvement phase 1	$(-8.92 \pm 3.61) \times 10^{-6}$	6.09	0.01
	β_4	Improvement phase 2	$(-2.11 \pm 0.78) \times 10^{-5}$	7.43	0.01
FA	β_1	Slope	$(-2.09 \pm 0.79) \times 10^{-3}$	6.97	0.01
	β_2	Improvement phase 1	$(3.40 \pm 1.94) \times 10^{-3}$	3.07	0.08
	β_4	Improvement phase 2	$(7.55 \pm 3.75) \times 10^{-3}$	4.06	0.05

Results of the nonlinear mixed effects model for each white matter metric in the full skeleton. The 2 improvement phases were estimated to begin during each training period. β_2 represents the degree of improvement relative to the slope in improvement phase 1. β_4 represents the degree of improvement relative to the slope in improvement phase 2. MD = mean diffusivity; AD = axial diffusivity; RD = radial diffusivity; FA = fractional anisotropy.

(decreased MD relative to the slope, β_2) was estimated to begin during the first training period (between time points 1 and 2), and to wear off during the subsequent rest period (between time points 2 and 3). The model further found a second improvement in MD (β_4), which was estimated to begin during the second training period (as shown by the turning point in the curve between time points 3 and 4), followed by a return towards the slope in the final rest period (between time points 4 and 5). A summary of the results is presented in Table 2.

The time courses of AD, RD, and FA are shown in Figure 3. The time courses of AD and RD showed similar results to those of MD, with a positive slope, indicating an increase in these metrics across the duration of the study. An improvement in AD and RD (decreased AD and RD relative to the slope, β_2) was estimated to begin during the first training period (between time points 1 and 2), and to wear off during the subsequent rest period (between time points 2 and 3). The model further found a second improvement in AD and RD (β_4), which was estimated to begin during the second training period (as shown by the turning point in the curve between time points 3 and 4), followed by a return towards the slope in the final rest period (between time points 4 and 5). The time course of FA showed variations corresponding to the opposite of those of MD, AD and RD. The slope function demonstrated a negative slope, indicating a general decrease in FA across the duration of the study. An improvement in FA (increased FA relative to the slope, β_2) was estimated to begin during the first training period (between time points 1 and 2), and to wear off during the subsequent rest period (between time points 2 and 3). The model further found a second improvement in FA (β_4), which was estimated to begin during the second training period (as shown by the turning point in the curve between time points 3 and 4), followed by a return towards the slope in the final rest period (between time points 4 and 5).

To compare the magnitude of WM microstructural changes in the 2 improvement phases, we first calculated the mean differences in MD and FA during each of the phases estimated by the model, and then calculated their z-score difference using the following equation:

$$(\delta_1 - \delta_2)/\sqrt{SE_{\delta_1}^2 + SE_{\delta_1}^2}.$$

The parameters δ_1 and δ_2 represent the magnitude of change in the model during each improvement phase. SE represents the standard errors. The 2 improvement phases did not differ for MD ($\delta_1 \pm SE = (0.93 \pm 4.05) \times 10^{-6}$, $\delta_2 = (7.24 \pm 8.79) \times 10^{-6}$, $z = -0.46$, $P = 0.64$) or FA ($\delta_1 = (-0.28 \pm 1.94) \times 10^{-3}$, $\delta_2 = (2.00 \pm 3.75) \times 10^{-3}$, $z = 0.30$, $P = 0.77$).

To investigate effects in specific tracts, the model was run on MD in the inferior frontal–occipital fasciculus (IFOF), inferior longitudinal fasciculus (ILF), superior longitudinal fasciculus (SLF), uncinate fasciculus (UF), and the hippocampal cingulum bundle (HCB), based on the JHU DTI-based WM atlas (Mori et al. 2005). Bonferroni's adjustment was applied to correct for multiple comparisons. The slope function demonstrated a positive slope for all the tracts (ILF: $\beta_1 = [7.00 \pm 1.90] \times 10^{-6}$, $F[1, 419] = 13.60$, $P = 2.56 \times 10^{-4}$, SLF: $\beta_1 = [5.49 \pm 1.69] \times 10^{-6}$, $F[1, 419] = 10.49$, $P = 0.001$, HCB; $\beta_1 = [1.42 \pm 0.39] \times 10^{-5}$, $F[1, 419] = 13.06$, $P = 3.38 \times 10^{-4}$; UF $\beta_1 = [6.08 \pm 2.47] \times 10^{-6}$, $F[1, 419] = 6.08$, $P = 0.01$, IFOF: $\beta_1 = [4.98 \pm 1.80] \times 10^{-6}$, $F[1, 419] = 7.64$, $P = 0.01$), indicating a general increase in MD across the duration of the study. An improvement in MD (decreased MD relative to the slope, β_2) was found in ILF ($\beta_2 = [-1.23 \pm 0.43] \times 10^{-5}$, $F[1, 419] = 8.41$, $P = 0.003$) and HCB ($\beta_2 = [-2.75 \pm 0.90] \times 10^{-5}$, $F[1, 419] = 9.20$, $P = 0.003$). This improvement was estimated to begin during the first training period (between time points 1 and 2), and to wear off during the subsequent rest period (between time points 2 and 3). In these tracts, the model further found a second improvement phase (β_4, ILF: $\beta_4 = [-2.85 \pm 0.95] \times 10^{-5}$, $F[1, 419] = 9.12$, $P = 0.003$, HCB: $\beta_4 = [-6.34 \pm 1.20] \times 10^{-5}$, $F[1, 419] = 10.51$, $P = 0.001$), which was estimated to begin during the second training period (as shown by the turning point in the curve between time points 3 and 4), followed by a return towards the slope in the final rest period (between time points 4 and 5). No significant MD improvements (α level for Bonferroni-corrected P-values = 0.01) were found for SLF ($\beta_2 = [-8.71 \pm 3.88] \times 10^{-6}$, $F[1, 419] = 5.03$, $P = 0.03$, $\beta_4 = [-1.71 \pm 0.84] \times 10^{-5}$, $F[1, 419] = 4.12$, $P = 0.04$), IFOF: $\beta_2 = [-6.85 \pm 4.16] \times 10^{-6}$, $F[1, 419] = 2.71$, $P = 0.10$, $\beta_4 = [-1.65 \pm 0.87] \times 10^{-5}$, $F[1, 419] = 3.62$, $P = 0.06$ and UF ($\beta_2 = [-9.09 \pm 5.89] \times 10^{-6}$, $F[1, 419] = 2.38$, $P = 0.12$, $\beta_4 = [-1.97 \pm 1.21] \times 10^{-5}$, $F[1, 419] = 2.63$, $P = 0.12$). The time course of MD in SLF and HCB is shown in Figure 4. The spatial locations of the tracts are shown in Figure 5.

The Time Course of Memory Performance

The time course of memory performance is shown in Figure 6. The model estimated 2 phases of memory improvement

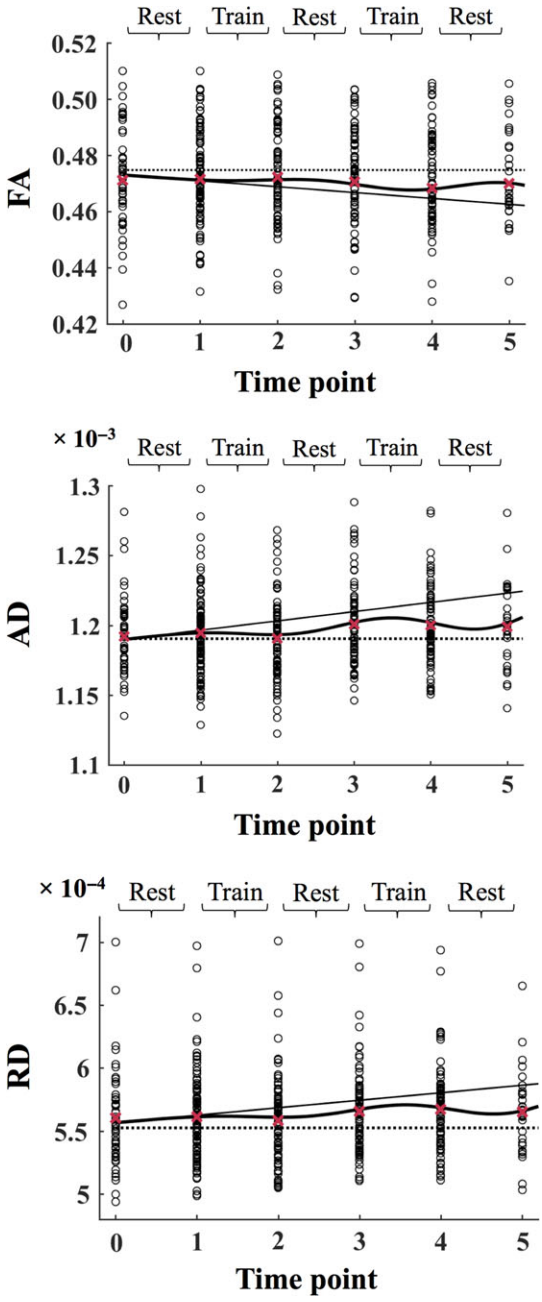

Figure 3. The AD, RD, and FA values for each subject are plotted separately at each time point. In each plot, the slope is displayed as a solid line, the full model is displayed as a solid curved line, and the dotted line marks the intercept of the model at time point 0. The mean values across all subjects are displayed as red crosses. The data is modeled according to Equation 1 (see Materials and Methods). FA = fractional anisotropy; AD = axial diffusivity; RD = radial diffusivity.

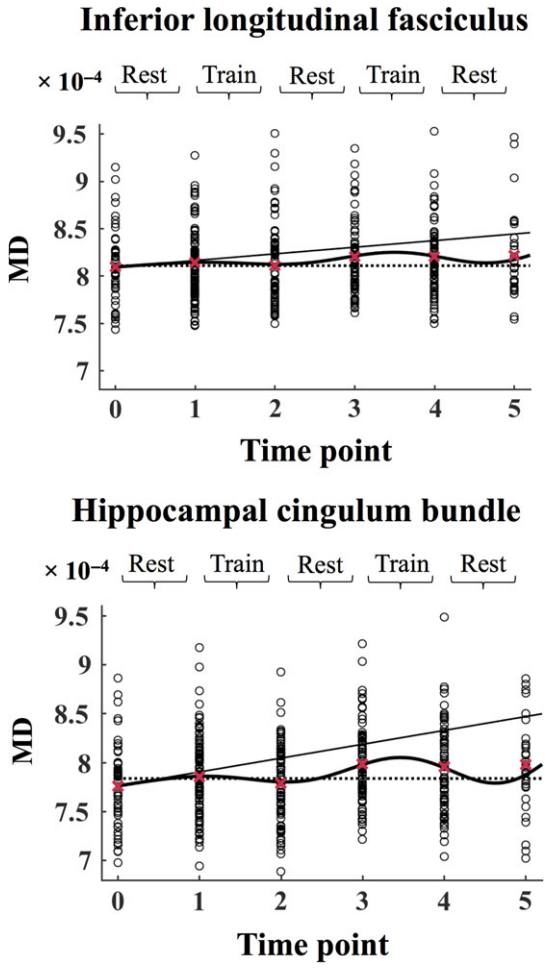

Figure 4. The MD values each subject in inferior longitudinal fasciculus and hippocampal cingulum bundle are plotted separately at each time point. In each plot, the slope is displayed as a solid line, the full model is displayed as a solid curved line, and the dotted line marks the intercept of the model at time point 0. The mean values across all subjects are displayed as red crosses. The data is modeled according to Equation 1 (see Materials and Methods). MD = mean diffusivity.

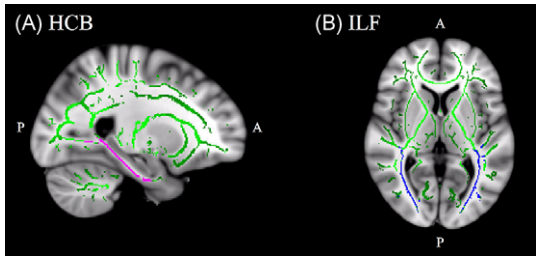

Figure 5. (A) Sagittal view of the hippocampal cingulum bundle, displayed in pink. Talairach coordinates x = 114, y = 123, z = 94, overlaid on the mean FA skeleton (green) and the standard MNI152 T1 mm^3 brain template. (B) Axial view of the inferior longitudinal fasciculus displayed in blue. Talairach coordinates x = 91, y = 115, z = 77, overlaid on the mean FA skeleton (green) and the standard MNI152 T1 mm^3 brain template.

relative to the intercept ($\beta_1 \pm$ SE = 10.62 ± 2.24, $F[1, 417] = 22.50$, $P = 2.89 \times 10^{-6}$, $\beta_3 = 10.84 \pm 4.51$, $F[1, 417] = 5.78$, $P = 0.02$), which corresponded to the phases of WM microstructural improvements. Memory performance changed significantly during the first improvement phase (mean change ± SE = 8.50 ± 1.05, $z = 5.71$, $P = 1.0 \times 10^{-05}$), while the change in performance was not significant during the second improvement phase (mean change ± SE = 2.01 ± 1.33, $z = 1.07$, $P = 0.28$). A comparison of the 2 improvement phases (using the same equation as for MD and FA) showed a larger memory change during the first improvement phase relative to the second ($z = 2.70$, $P = 0.007$).

Correlations between WM microstructure and memory performance at each time point of assessment showed no relationship between MD and memory performance at time point 0 ($r = 0.17$, $P = 0.30$), while negative relationships were observed between MD and memory performance at time points 1 ($r = -0.26$, $P = 0.01$),

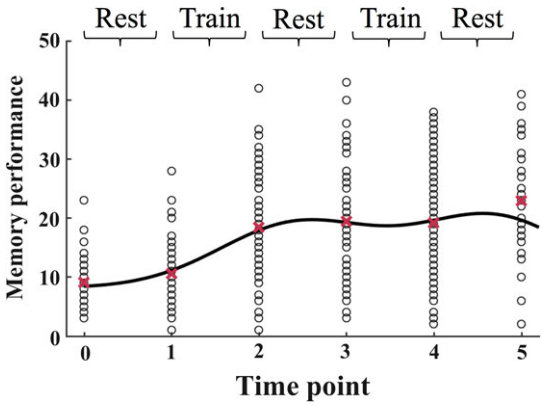

Figure 6. The memory performance values for each subject are plotted separately at each time point. The full model is displayed as a solid curved line, and the dotted line marks the intercept of the model at time point 0. The mean values across all subjects are displayed as red crosses. The data is modeled according to Equation 2 (see Materials and Methods).

2 ($r = -0.43$, $P = 4.8 \times 10^{-5}$), 3 ($r = -0.41$, $P = 2.2 \times 10^{-4}$), 4 ($r = -0.28$, $P = 0.01$), and 5 ($r = -0.34$, $P = 0.06$). No relationship was found between FA and memory performance at time point 0 ($r = 0.13$, $P = 0.40$), while positive relationships were found between FA and memory performance at time points 1 ($r = 0.31$, $P = 0.02$), 2 ($r = 0.42$, $P = 7.8 \times 10^{-5}$), 3 ($r = 0.40$, $P = 3.4 \times 10^{-4}$), 4 ($r = 0$ .34, $P = 0.01$), and 5 ($r = 0.36$, $P = 0.06$).

Discussion

The results show that targeted training interventions can influence WM microstructural trajectories in aging. Three main conclusions can be drawn: Firstly, the general decline in WM microstructure across the duration of the study was moderated following periods of training, demonstrating that cognitive training may promote a mitigating effect on age-related deterioration in brain structure. Secondly, the data were consistent with the model description of microstructural training effects subsiding over time. Hence, continuous training may be a premise for the enduring attenuation of neural decline. Finally, memory improvements were largely maintained after the initial training intervention. Thus, cognitive improvements may not rely on continuous training to the same degree as WM microstructure, which is consistent with previous findings (Driemeyer et al. 2008).

The improvements in both WM microstructure and memory performance at the final time point of assessment (time point 5, as visible by the means depicted in Figs. 2 and 6) could reflect a selection bias due to the drop-out rate. Lower cognitive performance among dropouts is commonly observed in longitudinal studies, resulting in a selection bias towards higher functioning individuals (Salthouse 2014). However, the group of individuals who completed the full study including time point 5, did not differ from the rest of the sample in terms of age, education, IQ, MMSE, and CVLT learning and recall, in addition to MD, FA, and performance on the 100-word test as measured at baseline (the results are provided in the Supplementary Material). Hence, although the decrease in sample size towards the end of the study could have affected the model precision, the remaining group of participants did not seem to represent a subsample of higher functioning individuals. As the function modeled continuous change rather than each interval as a slope, the onset and duration of the improvement phases were not forced to occur at the exact position of the measured time points of assessment. Hence, although the continuous function estimates a value at every point across the duration of the study, additional time points of assessment would have enabled a more precise description of the observed changes.

Although the physiological basis for water diffusion in WM is not fully understood (Beaulieu 2002), evidence suggests that WM microstructural decline is reflected by decreased FA and increased diffusivity, which is commonly observed in aging (Bennett and Madden 2014; Sexton et al. 2014). The memory training moderated the magnitude of the age-related decline in WM microstructure, corresponding to previous studies showing training-related microstructural plasticity in older adults (Lövdén , Bodammer, et al. 2010; Bennett et al. 2011; Engvig et al. 2012). DTI measurements reflect the restriction of water molecule motion, which can be imposed by cellular properties such as membranes, axonal density and myelin (Beaulieu 2002). While MD measures general diffusivity, AD and RD represent the rate of diffusion along the primary and secondary axes of the diffusion ellipsoid, respectively. FA measures the difference between the largest eigenvalue relative to the others, and has been associated with restricted molecular motion caused by directionally oriented microstructures such as myelin sheaths and axonal cell membranes (Pierpaoli et al. 1996; Beaulieu 2002).

The observed trajectories of MD, AD, and RD changes were accompanied by changes in FA in the opposite direction. Decreased MD, AD, and RD was accompanied by increased FA in the mitigation periods, while the opposite pattern was observed for the general slope across the duration of the study. Some evidence indicates that age-related decrease in FA is primarily driven by an increase in RD (Bhagat and Beaulieu 2004; Madden et al. 2009). Given the associations between both FA and RD and myelin in animal studies (Song et al. 2005; Blumenfeld-Katzir et al. 2011), the alterations in these metrics could be driven by changes in myelination. Recent animal studies have shown training-related increases in immunofluorescence staining of myelin basic protein, which is indicative of myelination, in co-occurrence with increased FA (Blumenfeld-Katzir et al. 2011; Sampaio-Baptista et al. 2013). Myelination is also suggested to be a central for human learning (Fields 2008, 2010). Although myelination may modulate the degree of anisotropy, evidence suggests that axonal membranes largely contribute to anisotropic diffusion (Beaulieu 2002). Thus, the changes in FA may also have been affected by the condition of axonal membranes. While the observed variations in AD could be associated with axonal alterations (Song et al. 2003), and the coherence of axonal orientation (Bennett IJ, DJ Madden, CJ Vaidya, DV Howard, and JH Howard, Jr. 2010), the changes in MD could indicate underlying alterations in relatively isotropic structures such as astrocytes (Blumenfeld et al. 2006; Sagi et al. 2012), which has been observed in animals after training (Blumenfeld-Katzir et al. 2011; Sagi et al. 2012). Alternatively, reduced MD may be driven by myelination of axons in crossing fiber regions (Mackey et al. 2012). Thus, the mechanisms underlying changes in DTI metrics depends upon the local fiber architecture. Clearly, signal changes from DTI require careful interpretation, as the exact neurobiological underpinnings of diffusion metrics cannot be directly inferred. Although DTI may be sensitive to underlying cellular changes of large enough volumetric contribution (Sagi et al. 2012; Fields 2015), the signal is also influenced by how axons are laid out within the voxel, as the gradients are applied along given axes (Jones et al. 2013). Diffusion measurements are also prone to cerebrospinal fluid

(CSF) based partial volume artefacts (Alexander et al. 2001; Metzler-Baddeley et al. 2012). As aging is associated with white and grey matter loss, the present study could benefit from corrections for CSF contamination to improve the precision of the WM measures. However, it has been reported that the commonly observed age-related differences in DTI metrics cannot be attributed to partial volume effects (Pfefferbaum and Sullivan 2003; Bhagat and Beaulieu 2004). The observed increases in MD, RD, and AD accompanied by decreased FA across the duration of the study are consistent with a number of cross-sectional and longitudinal studies showing corresponding patterns in DTI metrics in older age (Bennett et al 2010; Westlye et al. 2010; Sexton et al. 2014; Bender et al. 2016). Although some aging studies have indicated region-specific patterns of increased RD and reduced AD (Bennett et al. 2010; Burzynska et al. 2010), the predominant picture appears to be one of increased diffusivity in general. Changes in DTI metrics have previously been observed across periods of less than 3 months in older adults (Engvig et al. 2012), indicating that diffusion MRI is sensitive to short-term changes in microstructure. The general decline in WM microstructure across the study corresponded to the estimated annual change in a matched non-intervention sample, suggesting that age-related decline in WM microstructure is detectable over a period of less than a year.

As the cognitive processes involved in mnemonic strategies are likely to rely on multiple brain areas, efficient transfer and integration of information between these distributed regions is critical. Although the overall evidence does not currently demonstrate a high degree of regional specificity in the relationship between WM integrity and cognition (Madden et al. 2009; Salthouse 2011; Dresler et al. 2017), the observed differences in the extracted tracts indicate that the inferior longitudinal fasciculi and the hippocampal cingulum bundle may represent tracts of particular importance for information transfer that is beneficial for cognitive improvements after memory strategy training.

As evidence suggests that learning a new skill may affect brain structure to a greater extent relative to practicing those already learned (Driemeyer et al. 2008; Lövdén , Bäckman, et al. 2010), it is possible that a second training period comprising a new type of training could boost the neural mitigation to a larger extent. Thus, although beyond the scope of the present study, comparing the time course of plasticity in response to different training paradigms, for instance by also applying processed based working memory training (Karbach and Verhaeghen 2014), may represent a key focus for future research.

Conclusion

Targeted training has the potential to moderate the magnitude of age-related brain deterioration. The training-related improvements in WM microstructure were estimated to subside over time, indicating that continuous training may be a premise for the enduring attenuation of neural decline. Memory improvements from the initial training period were largely maintained across the duration of the study. Cognitive improvements may thus not rely on consistent training to the same degree as WM microstructure. In conclusion, the results suggest that continuous engagement in cognitive activities may influence brain-aging trajectories.

Supplementary Material

Supplementary material is available at *Cerebral Cortex* online.

Funding

This work was supported by the European Research Council's Starting Grant scheme (ERC grant agreement 313440 to K.B.W).

Notes

Conflict of Interest: None declared.

References

Alexander AL, Hasan KM, Lazar M, Tsuruda JS, Parker DL. 2001. Analysis of partial volume effects in diffusion-tensor MRI. Magn Reson Med. 45:770–780.

Andersson JL, Jenkinson M, Smith S. 2010. Non-linear registration, aka Spatial normalisation FMRIB technical report TR07JA2. FMRIB Analysis Group of the University of Oxford 2.

Andersson JL, Skare S, Ashburner J. 2003. How to correct susceptibility distortions in spin-echo echo-planar images: application to diffusion tensor imaging. NeuroImage. 20: 870–888.

Andersson JL, Sotiropoulos SN. 2016. An integrated approach to correction for off-resonance effects and subject movement in diffusion MR imaging. NeuroImage. 125:1063–1078.

Beaulieu C. 2002. The basis of anisotropic water diffusion in the nervous system—a technical review. NMR Biomed. 15: 435–455.

Behrens TE, Woolrich MW, Jenkinson M, Johansen-Berg H, Nunes RG, Clare S, Matthews PM, Brady JM, Smith SM. 2003. Characterization and propagation of uncertainty in diffusion-weighted MR imaging. Magn Reson Med. 50:1077–1088.

Bender AR, Volkle MC, Raz N. 2016. Differential aging of cerebral white matter in middle-aged and older adults: a seven-year follow-up. NeuroImage. 125:74–83.

Bennett IJ, Madden DJ. 2014. Disconnected aging: cerebral white matter integrity and age-related differences in cognition. Neuroscience. 276C:187–205.

Bennett IJ, Madden DJ, Vaidya CJ, Howard DV, Howard JH Jr. 2010. Age-related differences in multiple measures of white matter integrity: a diffusion tensor imaging study of healthy aging. Human Brain Mapp. 31:378–390.

Bennett IJ, Madden DJ, Vaidya CJ, Howard JH Jr, Howard DV. 2011. White matter integrity correlates of implicit sequence learning in healthy aging. Neurobiol Aging. 32:2317 e2311–2312.

Berlot R, Metzler-Baddeley C, Jones DK, O'Sullivan MJ. 2014. CSF contamination contributes to apparent microstructural alterations in mild cognitive impairment. NeuroImage. 92: 27–35.

Bhagat YA, Beaulieu C. 2004. Diffusion anisotropy in subcortical white matter and cortical gray matter: changes with aging and the role of CSF-suppression. J Magn Reson Imaging. 20: 216–227.

Blumenfeld B, Preminger S, Sagi D, Tsodyks M. 2006. Dynamics of memory representations in networks with novelty-facilitated synaptic plasticity. Neuron. 52:383–394.

Blumenfeld-Katzir T, Pasternak O, Dagan M, Assaf Y. 2011. Diffusion MRI of structural brain plasticity induced by a learning and memory task. PLoS One. 6:e20678.

Bower GH. 1970. Analysis of a mnemonic device. Am Sci. 58: 496–510.

Boyke J, Driemeyer J, Gaser C, Buchel C, May A. 2008. Training-induced brain structure changes in the elderly. J Neurosci. 28:7031–7035.

Burnham KP, Anderson DR. 2003. Model selection and multimodel inference: a practical information-theoretic approach. New York: Springer Science & Business Media.

Burzynska AZ, Preuschhof C, Bäckman L, Nyberg L, Li S-C, Lindenberger U, Heekeren HR. 2010. Age-related differences in white matter microstructure: region-specific patterns of diffusivity. NeuroImage. 49:2104–2112.

Cavallini E, Pagnin A, Vecchi T. 2003. Aging and everyday memory: the beneficial effect of memory training. Arch Gerontol Geriatr. 37:241–257.

de Lange AG, Brathen AC, Grydeland H, Sexton C, Johansen-Berg H, Andersson JL, Rohani DA, Nyberg L, Fjell AM, Walhovd KB. 2016. White matter integrity as a marker for cognitive plasticity in aging. Neurobiol Aging. 47:74–82.

de Lange AMG, Bråthen ACS, Rohani DA, Grydeland H, Fjell AM, Walhovd KB. 2017. The effects of memory training on behavioral and microstructural plasticity in young and older adults. Hum Brain Mapp. 38:5666–5680.

Delis DC, Kramer JH, Kaplan E, Ober BA. 2000. California verbal learning test. 2nd ed. (CVLT-II). San Antonio, TX: The Psychological Corporation.

Draganski B, Gaser C, Busch V, Schuierer G, Bogdahn U, May A. 2004. Neuroplasticity: changes in grey matter induced by training. Nature. 427:311–312.

Dresler M, Shirer WR, Konrad BN, Müller NC, Wagner IC, Fernández G, Czisch M, Greicius MD. 2017. Mnemonic training reshapes brain networks to support superior memory. Neuron. 93:1227–1235. e1226.

Driemeyer J, Boyke J, Gaser C, Buchel C, May A. 2008. Changes in gray matter induced by learning—revisited. PLoS One. 3: e2669.

Engvig A, Fjell AM, Westlye LT, Moberget T, Sundseth O, Larsen VA, Walhovd KB. 2010. Effects of memory training on cortical thickness in the elderly. NeuroImage. 52:1667–1676.

Engvig A, Fjell AM, Westlye LT, Moberget T, Sundseth O, Larsen VA, Walhovd KB. 2012. Memory training impacts short-term changes in aging white matter: a longitudinal diffusion tensor imaging study. Human Brain Mapp. 33:2390–2406.

Fields RD. 2008. White matter in learning, cognition and psychiatric disorders. Trends Neurosci. 31:361–370.

Fields RD. 2010. Change in the brain's white matter. Science. 330:768–769.

Fields RD. 2015. A new mechanism of nervous system plasticity: activity-dependent myelination. Nat Rev Neurosci. 16: 756–767.

Folstein MF, Folstein SE, McHugh PR. 1975. "Mini-mental state". A practical method for grading the cognitive state of patients for the clinician. J Psychiatr Res. 12:189–198.

Jones DK, Knosche TR, Turner R. 2013. White matter integrity, fiber count, and other fallacies: the do's and don'ts of diffusion MRI. NeuroImage. 73:239–254.

Karbach J, Verhaeghen P. 2014. Making working memory work: a meta-analysis of executive-control and working memory training in older adults. Psychol Sci. 25:2027–2037.

Lezak MD. 2004. Neuropsychological assessment. USA: Oxford University Press.

Little RJ, Rubin DB. 2014. Statistical analysis with missing data. Hoboken, NJ: John Wiley & Sons.

Lövdén M, Bodammer NC, Kuhn S, Kaufmann J, Schutze H, Tempelmann C, Heinze HJ, Duzel E, Schmiedek F, Lindenberger U. 2010. Experience-dependent plasticity of white-matter microstructure extends into old age. Neuropsychologia. 48: 3878–3883.

Lövdén M, Bäckman L, Lindenberger U, Schaefer S, Schmiedek F. 2010. A theoretical framework for the study of adult cognitive plasticity. Psychol Bull. 136:659–676.

Mackey AP, Whitaker KJ, Bunge SA. 2012. Experience-dependent plasticity in white matter microstructure: reasoning training alters structural connectivity. Front Neuroanat. 6:32.

Madden DJ, Bennett IJ, Song AW. 2009. Cerebral white matter integrity and cognitive aging: contributions from diffusion tensor imaging. Neuropsychol Rev. 19:415–435.

Metzler-Baddeley C, O'Sullivan MJ, Bells S, Pasternak O, Jones DK. 2012. How and how not to correct for CSF-contamination in diffusion MRI. NeuroImage. 59:1394–1403.

Mori S, Wakana S, Van Zijl PC, Nagae-Poetscher L. 2005. MRI atlas of human white matter. Amsterdam: Elsevier.

Pfefferbaum A, Sullivan EV. 2003. Increased brain white matter diffusivity in normal adult aging: relationship to anisotropy and partial voluming. Magn Reson Med. 49:953–961.

Pierpaoli C, Jezzard P, Basser PJ, Barnett A, Di Chiro G. 1996. Diffusion tensor MR imaging of the human brain. Radiology. 201:637–648.

Rueckert D, Sonoda LI, Hayes C, Hill DLG, Leach MO, Hawkes DJ. 1999. Nonrigid registration using free-form deformations: application to breast MR images. IEEE Trans Med Imaging. 18:712–721.

Sagi Y, Tavor I, Hofstetter S, Tzur-Moryosef S, Blumenfeld-Katzir T, Assaf Y. 2012. Learning in the fast lane: new insights into neuroplasticity. Neuron. 73:1195–1203.

Salthouse TA. 2011. Neuroanatomical substrates of age-related cognitive decline. Psychol Bull. 137:753–784.

Salthouse TA. 2014. Selectivity of attrition in longitudinal studies of cognitive functioning. J Gerontol B Psychol Sci Soc Sci. 69:567–574.

Sampaio-Baptista C, Khrapitchev AA, Foxley S, Schlagheck T, Scholz J, Jbabdi S, DeLuca GC, Miller KL, Taylor A, Thomas N, et al. 2013. Motor skill learning induces changes in white matter microstructure and myelination. J Neurosci. 33:19499–19503.

Scholz J, Klein MC, Behrens TE, Johansen-Berg H. 2009. Training induces changes in white-matter architecture. Nat Neurosci. 12:1370–1371.

Sexton CE, Walhovd KB, Storsve AB, Tamnes CK, Westlye LT, Johansen-Berg H, Fjell AM. 2014. Accelerated changes in white matter microstructure during aging: a longitudinal diffusion tensor imaging study. J Neurosci. 34:15425–15436.

Smith SM. 2002. Fast robust automated brain extraction. Hum Brain Mapp. 17:143–155.

Smith SM, Jenkinson M, Johansen-Berg H, Rueckert D, Nichols TE, Mackay CE, Watkins KE, Ciccarelli O, Cader MZ, Matthews PM, et al. 2006. Tract-based spatial statistics: voxelwise analysis of multi-subject diffusion data. NeuroImage. 31:1487–1505.

Song SK, Sun SW, Ju WK, Lin SJ, Cross AH, Neufeld AH. 2003. Diffusion tensor imaging detects and differentiates axon and myelin degeneration in mouse optic nerve after retinal ischemia. NeuroImage. 20:1714–1722.

Song SK, Yoshino J, Le TQ, Lin SJ, Sun SW, Cross AH, Armstrong RC. 2005. Demyelination increases radial diffusivity in corpus callosum of mouse brain. NeuroImage. 26:132–140.

Wechsler D. 1999. Wechsler abbreviated scale of intelligence. San Antonio, TX: The Psychological Corporation.

Westlye LT, Walhovd KB, Dale AM, Bjornerud A, Due-Tonnessen P, Engvig A, Grydeland H, Tamnes CK, Ostby Y, Fjell AM. 2010. Life-span changes of the human brain white matter: diffusion tensor imaging (DTI) and volumetry. Cereb Cortex. 20:2055–2068.